Inelastic scattering of ^{3}He from samarium isotopes at 53 MeV

R. Eagle

Bedford College, Regent's Park, London NW1, United Kingdom

N. M. Clarke and R. J. Griffiths

Wheatstone Laboratory, King's College, Strand, London WC2R 2LS, United Kingdom

C. B. Fulmer and D. C. Hensley

Oak Ridge National Laboratory, * *Oak Ridge, Tennessee 37830*

(Received 16 May 1977)

Angular distributions of ^{3}He inelastic scattering from the stable even isotopes of samarium were measured at an incident particle energy of 53.4 MeV. The data for 2^+ and 3^- collective states extend to 150° for ^{144,148,150}Sm and to 100° for 2^+ states in ^{152,154}Sm. The cross sections span approximately seven orders of magnitude. The data were analyzed with the distorted-wave Born approximation and the strong-coupling approximation. Quadrupole and octopole deformation parameters thus obtained are compared with results from analyses of proton and α-particle-scattering data.

$$\left[\begin{array}{c} \text{NUCLEAR REACTIONS} \quad ^{144,\,148,\,150,\,152,\,154}\text{Sm}(^3\text{He}, {}^3\text{He}')\ E_{3\text{He}} = 53.4 \text{ MeV, mea-} \\ \text{sured } \sigma(\theta) \text{ for } 2^+ \text{ and } 3^- \text{ states, DWBA and SCA analyses, deduced deforma-} \\ \text{tion parameters.} \end{array} \right]$$

INTRODUCTION

In this paper we report a study of inelastic scattering of ^{3}He from the stable even isotopes of samarium.[1] These targets are an interesting group for studying the collective motions of nuclei. They span the transition from a major closed neutron shell (^{144}Sm) through vibrational nuclei and into the rare earth region of permanent deformation. In inelastic scattering they exhibit strongly excited 2^+ and 3^- levels with level spacings characteristic of a vibrational band for the ^{144}Sm, ^{148}Sm, and ^{150}Sm isotopes and of a rotational band for ^{152}Sm and ^{154}Sm. The excitation of these levels provides information on the deformations that occur in these collective motions.

Previous elastic- and inelastic-scattering measurements and analyses for samarium isotopes have been reported for protons at 50 MeV[2(a),2(b)] and at 16 MeV,[3,4] and for α particles[5,6] at 50 MeV. The present measurements on ^{148}Sm, ^{150}Sm, ^{152}Sm, and ^{154}Sm with ^{3}He particles were made at 53.4 MeV and supplement the measurements on ^{144}Sm already reported.[7]

The measurements on ^{148}Sm and ^{150}Sm were performed with ΔE-E telescopes of silicon surface barrier detectors at the variable energy cyclotron at United Kingdom Atomic Energy Authority Harwell where the beam intensity of up to 1800 nA on target facilitated measurements at angles as large as 150°. The measurements on ^{152}Sm and ^{154}Sm required high resolution to separate the first excited

states (122 and 82 keV, respectively) and hence were performed with the broad range magnetic spectrometer at the Oak Ridge isochronous cyclotron. The lower beam intensity and smaller solid angle limited the latter measurements to angles $< 100°$.

In an earlier paper[8] the elastic-scattering cross sections were presented together with a conventional optical-model analysis which investigated various discrete and continuous ambiguities in the potentials. The preferred potentials were those with real volume integrals per particle pair, J_R, ~300 MeV fm^3 and included a surface absorption term; addition of volume absorption and spin orbit terms to the potentials did not result in improved fits to the data. The potentials were characterized by large radii and diffuseness of the absorption potential in agreement with other work at 40 MeV.[9]

In the optical-model analyses of the elastic data[8] the parameter sets obtained showed only slight variations in the well depths (except for the potential family characterized by J_R~240 MeV fm^3). A folding model calculation[10] demonstrated that variations observed could be adequately explained by the density dependence of the effective interaction. The similarity of the potentials for the range of isotopes suggested that it may be possible to describe the inelastic-scattering angular distributions for the range of isotopes with a single optical-model potential by varying only the deformation parameters. This approach, which is based on the assumption that the principal difference in the iso-

topes is in their strongly excited collective levels, was successful in describing α-particle inelastic scattering.[5,6] The α-particle data, however, were limited to angles forward of 80°, and the same approach was not so successful on the more extensive proton data.[2]

DISTORTED-WAVE BORN APPROXIMATION ANALYSIS

The inelastic-scattering data were first analyzed with a conventional distorted-wave Born-approximation (DWBA) approach using the code DWUCK.[11] In the formalism of the collective model a distorted nucleus is represented by an axially symmetric nonspherical surface given by

$$R(\theta) = R_0\left(1 + \sum_l \beta_l Y_l^0(\theta)\right). \tag{1}$$

The coupling between the ground state and the excited levels is assumed to be weak so that an expansion of the potential in terms of the deformation parameters β_l becomes, e.g., for the first 2^+ level

$$V[r - R(\theta)] = V(r - R_0) - \beta_2 Y_2^0(\theta)\frac{dV}{dr}, \tag{2}$$

where $V(r - R_0)$ is the optical-model potential for elastic scattering. The inelastic scattering is accounted for by the radial derivative term. For inelastic scattering from the lowest 2^+ level of even nuclei DWUCK predicts differential cross sections related to the data by

$$\left(\frac{d\sigma}{d\Omega}\right)_{exp} = \beta_2^2\left(\frac{d\sigma}{d\Omega}\right)_{DWUCK}. \tag{3}$$

The calculated angular distributions are normalized to the data by a least squares fit to obtain values of β_2. In this analysis, βR for Coulomb and nuclear interactions are essentially the same.

The present DWBA analyses were performed with three sets of optical-model potentials (from Ref. 8) characterized by $J_R \sim 240$, 300, and 400 MeV fm³, where $J_R = (1/A_p A_T)4\pi V_R \int r^2 f(r)dr$ [$f(r)$ is the radial form factor]. The resulting fits to the 2^+ levels for all five target isotopes and to the 3^- levels of ¹⁴⁴Sm, ¹⁴⁸Sm, and ¹⁵⁰Sm are presented in Figs. 1 and 2, respectively. The corresponding values of β_2 and β_3 are given in Table I.

The quality of the DWBA fits is equally good for all three potentials so inelastic-scattering data (at 53.4 MeV) do not confirm the preference for the potential with $J_R \sim 300$ MeV fm³ that was indicated from analysis of data at higher energy.[12]

For all three potentials the DWBA predictions differ appreciably from the data at the most forward angles. This is a puzzling result. The question of whether enough partial waves were used in the calculation was considered. The usual re-
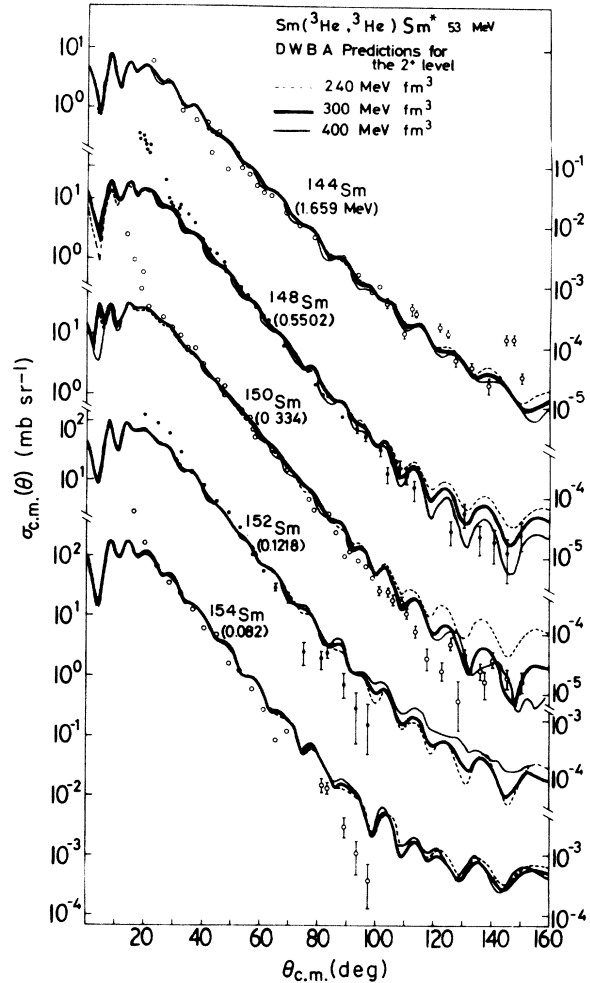
FIG. 1. Angular distributions for inelastic scattering of 53.4 MeV ³He to the first 2^+ levels of the stable even isotope of samarium. The DWBA calculations were with sets of optical-model parameters (from Ref. 8) for which $J_R \sim 240$, 300, and 400 MeV fm³.

quirement if Coulomb excitation is included is that l_{max} be at least as large as $2\eta/\theta_{min}$ where η is the Coulomb parameter $(Z_1 Z_2 e^2/\hbar v)$ and θ_{min} is the smallest angle, in radians, at which calculations are made. For the present situation for $\theta_{min} = 8°$ this indicates $l_{max} \sim 70$ should be used. The DWBA calculations used this value. Repeating some of the calculations with l_{max} increased by 50% yielded no significant differences in the predicted angular distributions. The DWBA calculations were also checked by comparing the results with those of other codes and computers and the differences were found to be very small. The data for ¹⁵²,¹⁵⁴Sm were obtained with an experimental arrangement appreciably different from that used for the other targets. It is thus unlikely that systematic experimental errors are the cause of the lack of agreement between the data and the calculated angular

TABLE I. Deformation parameters obtained from DWBA analyses using optical-model potentials with $J_R \sim 240$, 300, and 400 MeV fm³ (sets A, B, and C, respectively). The potential sets are from Ref. 8.

Deformation	Potential set	^{144}Sm	^{148}Sm	^{150}Sm	^{152}Sm	^{154}Sm
β_2	A	0.099	0.136	0.169	0.287	0.369
β_2	B	0.075	0.128	0.176	0.276	0.367
β_2	C	0.095	0.137	0.168	0.277	0.380
β_3	A	0.115	0.139	0.136		
β_3	B	0.114	0.155	0.129		
β_3	C	0.114	0.156	0.136		

distributions at very forward angles.

The values of β_2 and β_3 obtained from the DWBA fits (Table I) do not vary appreciably for the three parameter sets used. In all cases the values of β_2 obtained in the present analysis of ³He scattering are a little larger than those obtained in previous (p,p'),[2-4] and (α, α')[5,6] work. The values obtained from $B(E2)$ measurements[13] (for [148,150,152]Sm) are very close to those obtained in our DWBA analysis; the closest agreement is with β_2 values obtained with parameter set B, i.e., $J_R \sim 300$ MeV fm³. In all cases the β_2 values in-

crease with target mass while the octopole deformation parameter, β_3, for ^{148}Sm appears to be larger than that of ^{150}Sm. This is also observed in the coupled-channels analysis described below.

COUPLED-CHANNEL ANALYSIS

The strong-coupling approach (SCA) extends the optical-model potential to include a permanent spheroidal deformation which generates coupled radial equations when introduced into the Schrödinger equation. The present SCA analyses were performed principally with the code JUPITOR-KARLSRUHE[14] using the IBM 195 computer at the Rutherford Laboratory. Optical-model potentials with $J_R \sim 300$ MeV fm³ were used throughout with surface absorption and without a spin-orbit term. For the isotopes [144,148,150]Sm a vibrational model coupling of the 0⁺, 2⁺, and 3⁻ states was used and for [152,154]Sm a rotational model coupling 0⁺, 2⁺ (and in some cases 4⁺) states was used, although data existed for only the 0⁺ and 2⁺ states. All of the calculations employed ~70 partial waves and
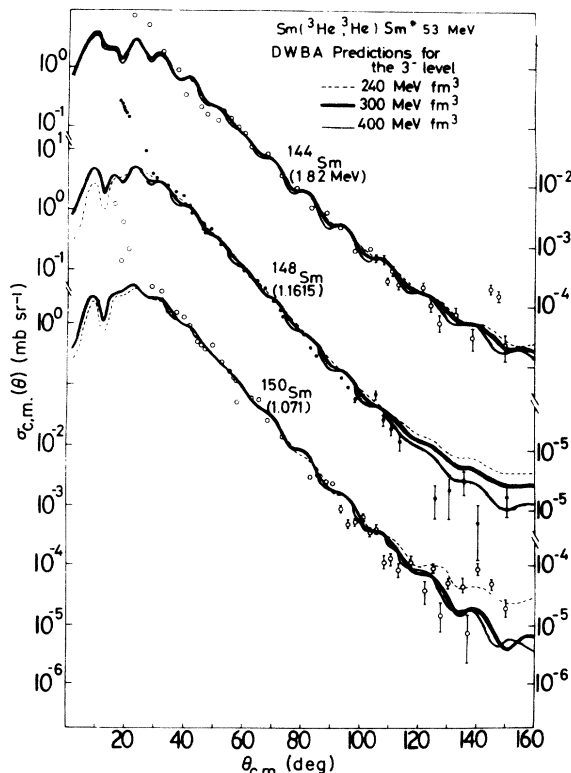
FIG. 2. Angular distributions for inelastic scattering of 53.4 MeV ³He to the first 3⁻ states of the stable even vibrational isotopes of samarium. The DWBA predictions are from the calculations referred to in Fig. 1.

TABLE II. Parameters obtained from an SCA analysis of ³He inelastic-scattering data from ^{144}Sm. The real radius parameter r_R was fixed at 1.136 fm (from Ref. 7). Coupling 0⁺ and 2⁺ states yielded set a and coupling 0⁺, 2⁺, and 3⁻ states yielded set b. All well depths are in MeV and all geometrical parameters are in fm. Values of χ^2 per point are listed.

Parameter	Set a	Set b
V_R	137.1	132.2
a_R	0.79	0.81
W_D	28.1	27.4
r_D	1.18	1.20
a_D	0.87	0.82
β_2	0.077	0.076
β_3		0.09
$\chi^2(0^+)$	30	37
$\chi^2(2^+)$	65	67
$\chi^2(3^-)$		81
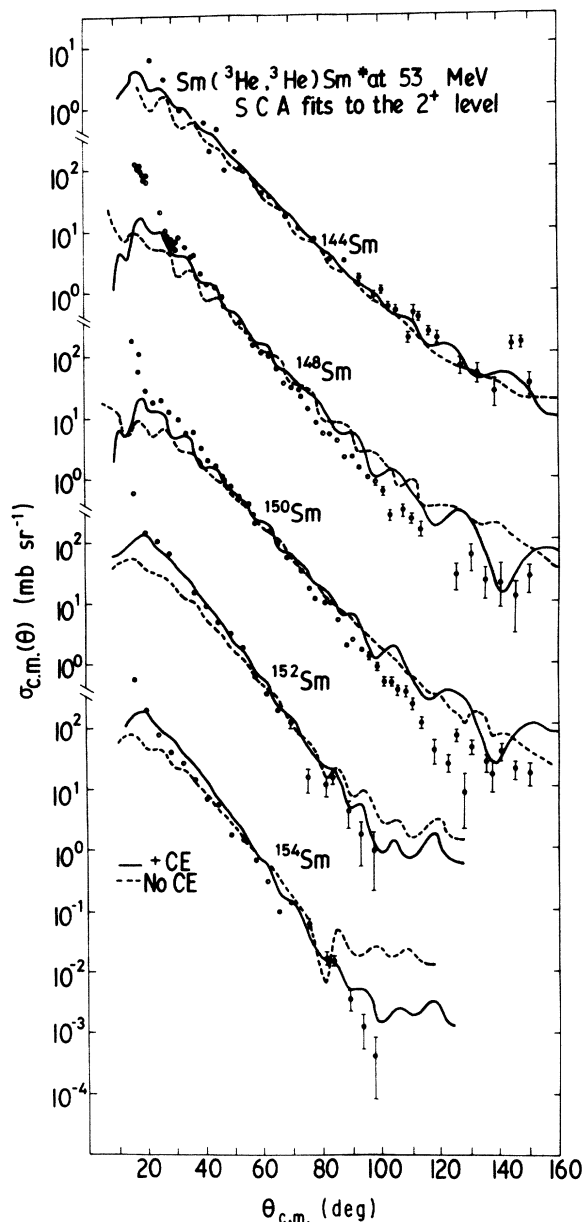
FIG. 3. Angular distributions for inelastic scattering
of 53.4 MeV ³He to the first 2⁺ levels of the stable even
isotopes of samarium. The couplings used and results
of the SCA fits are given in Table III.

FIG. 4. Angular distributions for inelastic scattering
of 53.4 MeV ³He to the first 3⁻ states of the stable even
vibrational isotopes of samarium. The SCA fits were
obtained simultaneously with those of Figs. 3 and 5.

integration of the radial equations extended out to
25 fm. Both real and imaginary potentials and the
Coulomb potential were deformed and calculations
were performed with and without Coulomb excita-
tion being included.

For comparison a number of the SCA calculations
were repeated (without parameter searching) with
the code ECIS73 [15] using the IBM 360/91 computer
at Oak Ridge National Laboratory. For these cal-
culations ~100 partial waves were used when Cou-

lomb excitation was included and ~40 partial waves
(the actual value of l_{max} was determined for each
case by the code) when Coulomb excitation was not
included. Integration of the radial equations was in
steps of ~0.18 fm and extended to 40 fm. For all
of the calculations with ECIS73 the predicted angu-
lar distributions are in good agreement with those
obtained with the code JUPITOR-KARLSRUHE. Re-
sults of the latter are presented below.
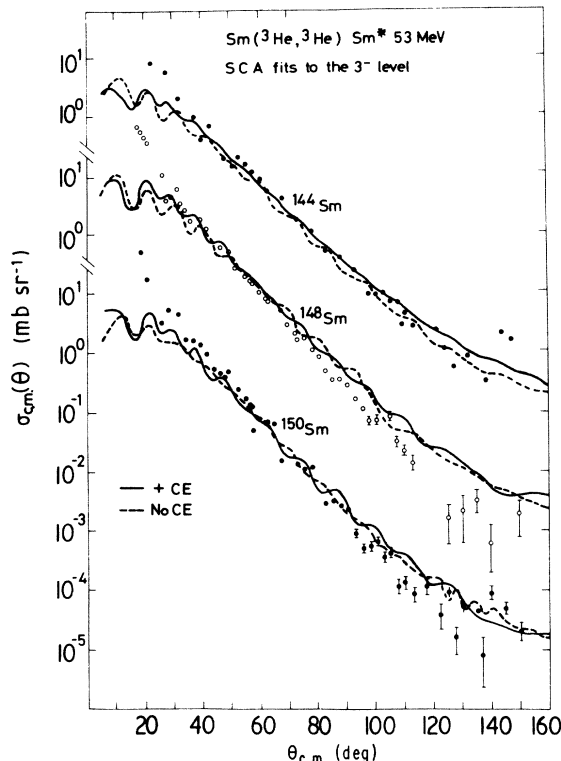
The initial SCA analyses used the ¹⁴⁴Sm data of
Ref. 7 and all of the parameters were allowed to
vary except the real radius parameter which was
fixed at 1.136 fm. The resulting parameters are
listed in Table II; set a was obtained by coupling
the 0⁺ and 2⁺ states and set b was obtained when
0⁺, 2⁺, and 3⁻ states were coupled. There are
only slight variations in the values of individual
parameters thus obtained from the two searches
with different coupling. The geometry parameters
of set b were then used as fixed parameters in
searches on the other data sets with the well
depths and deformations as variable parameters.
Table III lists the resulting values of the param-
eters and the corresponding fits to the data are
shown in Figs. 3–5. In Table III and below in
Table IV values of χ^2 (computed in the usual way)

TABLE III. Well depths and deformation parameters obtained from SCA analyses of inelastic ^{3}He scattering from samarium isotopes with fixed geometry parameters (set b of Table II). For ^{144,148,150}Sm 0$^+$, 2$^+$, and 3$^-$ states were coupled, for ^{152,154}Sm 0$^+$, 2$^+$, and 4$^+$ states were coupled. For ^{152,154}Sm values of β_4 (0.048 and 0.054, respectively) and β_6 (−0.012 and −0.018, respectively) from Ref. 5 were used. A and B, respectively, imply Coulomb excitation not included and included. Values of χ^2 per point are listed.

		V_R	W_D	β_2	β_3	$\chi^2(0^+)$	$\chi^2(2^+)$	$\chi^2(3^-)$
^{144}Sm	A	132.2	27.4	0.076	0.090	37	67	81
	B	121.8	33.4	0.063	0.087	168	16	16
^{148}Sm	A	139.9	26.3	0.138	0.133	88	392	237
	B	142.1	29.3	0.126	0.128	293	306	197
^{150}Sm	A	133.4	24.8	0.162	0.103	125	347	187
	B	127.0	25.0	0.140	0.105	154	356	175
^{152}Sm	A	128.4	24.4	0.337		31	216	
	B	132.2	27.4	0.346		69	74	
^{154}Sm	A	129.7	25.5	0.387		30	473	
	B	132.2	27.4	0.389		611	235	
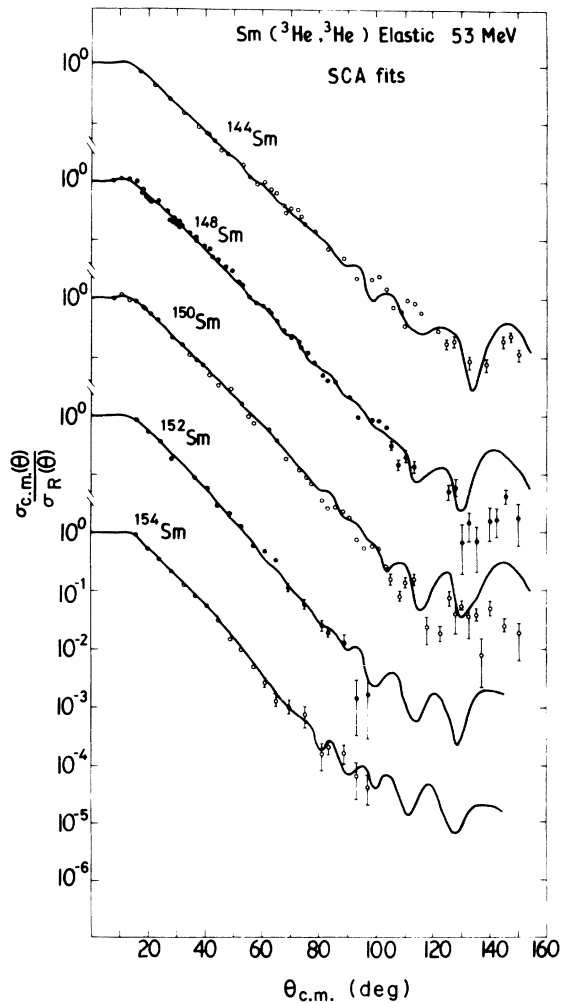
FIG. 5. Angular distributions of elastic scattering of 53.4 MeV ^{3}He from the stable even isotopes of samarium. The SCA fits were obtained simultaneously with those of Figs. 3 and 4.

are listed for the various experimental angular distributions. These have most meaning for the elastic-scattering data but are included for the inelastic data as some means of comparing results from different coupling schemes, geometry, etc.

For ^{152,154}Sm the 4$^+$ states were explicitly coupled in the calculations although no data were available and β_4 was not varied. Values of β_4 and β_6 listed in Table III are those from the α-particle work of Hendrie et al.[5] to provide some comparison of the β_2 values. Since β_2 values in Table III are somewhat larger than those obtained in the work of Hendrie et al. ($\beta_2 = 0.13$, 0.246, and 0.270, respectively, for ^{148}Sm, ^{152}Sm, and ^{154}Sm) it is probable that, given 4$^+$ and 6$^+$ ^{3}He data, different values of β_4 and β_6 might have been obtained. The values, however, are not large and we feel this approximation is reasonable.

As in the case of DWBA calculations angular distributions predicted for inelastic scattering to the 2$^+$ level by the SCA differ appreciably from the data at the most forward angles. The agreement is improved for each of the five targets by including Coulomb excitation in the calculation but good fits are still not obtained at the most forward angles. The fits to the large angle ($\theta > 100°$) data for ^{144,148,150}Sm, where cross sections are $\lesssim 100$ nb/sr, are not as good for the SCA as for the DWBA calculations. In spite of difficulties at both small and large angles the SCA calculations are in fair agreement with the measured angular distributions (in which the cross sections span seven orders of magnitude) and yield β_2 values to compare with those from earlier SCA analyses of data from scattering of different particles.

The SCA fits to the 3$^-$ angular distributions (Fig. 4) also reproduce the general features of the data

but the fits are poor at both the most forward and most backward angular regions. In contrast to the 2⁺ results including Coulomb excitation in the calculations results in only slight changes in the predicted 3⁻ angular distributions that do not improve the fits at either small or large angles.

The SCA calculations of the elastic scattering reproduce the gross features of the data reasonably well, but in detail the fits (Fig. 5) are not as good as those obtained in the optical-model analyses of Ref. 8. In particular, the small oscillations in the experimental angular distributions (for $\theta < 100°$) are not reproduced as well in the SCA analysis as in the optical-model analysis. At large angles, where the cross sections are very small (≤ 100 nb/sr) angular distributions from the SCA calculations differ from those of the optical model but the qualitative agreement with the data is about equal for the two.

The SCA calculations of the elastic-scattering angular distributions shown in Fig. 5 do not include Coulomb excitation. When it is included in the SCA calculations the agreement with the elastic-scattering data is poorer than when it is not included. Thus we have the result that including Coulomb excitation in the SCA calculation worsens the fit to the elastic scattering, improves it to 2⁺ inelastic scattering, and makes little difference for 3⁻ inelastic scattering.

For each of the target nuclei a search was performed in which all of the parameters except r_R were varied. To reduce the amount of computing time coupling of the 4⁺ levels of ¹⁵²,¹⁵⁴Sm was not included but Coulomb excitation was included for these nuclei since it is of increasing importance as the energy of the 2⁺ state is lowered. Coulomb excitation was not included for ¹⁴⁴,¹⁴⁸,¹⁵⁰Sm, however. Table IV shows the values of the parameters thus obtained. With the variable geometry

the fits to the 2⁺ angular distributions for ¹⁵²,¹⁵⁴Sm are as good as or better than those obtained above in fixed-geometry searches which included coupling of the 4⁺ level.

DISCUSSION

The ³He data analyzed in the present work are distinctly different in two ways from those used in previously reported analyses of inelastic scattering of protons[2,4] and α particles[5,6] from the samarium isotopes. The ³He cross sections span six to seven orders of magnitude in contrast to three or less for the proton and α-particle data, and the angular distributions exhibit very little structure in contrast to those for protons and α particles. The latter feature was a problem in fitting the ³He data, particularly the elastic scattering,[8] because the real potential would frequently "jump" to another "discrete potential family."

The lack of structure in the angular distributions resulted in low sensitivity of the calculations to values of the optical-model parameters. This is apparent if one compares χ^2 values in Table III (from fixed geometry searches) with the corresponding χ^2 values in Table IV (from variable geometry searches). Table I also shows (for DWBA calculations) only small variations of deformation parameters for three discrete families of optical-model potential.

In the SCA parameter searches the values of the well depths are reasonably uniform both in the fixed geometry and in the variable geometry fits. The values obtained for V_R in both SCA analyses are not significantly different from those obtained in the optical-model analyses (Ref. 8) with $J_R \sim 300$ MeV fm³. Only for ¹⁵⁴Sm are the values of W_D significantly lower in the SCA analyses compared to the optical-model analysis. The most pronounced

TABLE IV. Parameters obtained from SCA analyses of inelastic ³He scattering from samarium isotopes with variable geometry parameters (r_R was fixed at 1.136 fm). For ¹⁴⁴,¹⁴⁸,¹⁵⁰Sm 0⁺, 2⁺, and 3⁻ states were coupled and Coulomb excitation was not included. For ¹⁵²,¹⁵⁴Sm 0⁺ and 2⁺ states were coupled and Coulomb excitation was included. Values of χ^2 per point are listed.

Parameter	¹⁴⁴Sm	¹⁴⁸Sm	¹⁵⁰Sm	¹⁵²Sm	¹⁵⁴Sm
V_R	132.2	138.6	133.5	130.9	141.7
a_R	0.808	0.765	0.769	0.646	0.618
W_D	27.4	23.2	24.8	27.2	18.8
r_D	1.20	1.16	1.16	0.941	0.897
a_D	0.821	0.941	0.944	1.15	1.27
β_2	0.076	0.143	0.163	0.325	0.44
β_3	0.090	0.127	0.104		
$\chi^2(0^+)$	37	96	124	76	72
$\chi^2(2^+)$	67	359	348	81	146
$\chi^2(3^-)$	81	319	186		
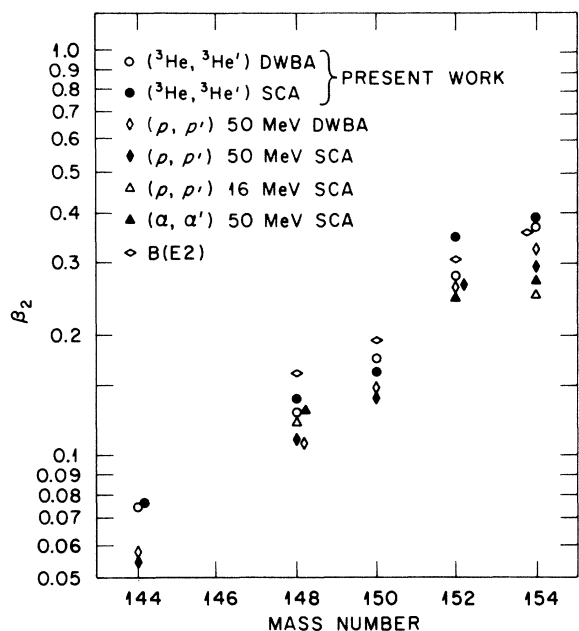
FIG. 6. Quadrupole deformation parameters of the stable even isotopes of samarium. The DWBA results are from potential set B of Table I. The SCA results for (^{3}He, ^{3}He$'$) are from the fixed geometry analyses summarized in Table III; for both a Coulomb radius parameter of 1.25 fm was used. The 50 MeV (p,p') results are from Ref. 2, the 16 MeV (p,p') results are from Ref. 4, the (α, α') results are from Ref. 5, and the $B(E2)$ results from Ref. 13 were converted using $R = 1.2A^{1/3}$. A few of the plotted points are slightly displaced horizontally for clarity.

FIG. 7. Octopole deformation parameters of the stable even vibrational isotopes of samarium. The (^{3}He, ^{3}He$'$) results are from the same analyses as those of Fig. 6. The 16 MeV (p,p') result is from Ref. 4.

trend in the parameters is in the decrease of r_D and the increase of a_D as the target mass changes from the vibrational region to the rotational region. There is also a distinct difference in a_R (opposite from that of a_D) for vibrational and rotational nuclei. In the optical-model analyses of the elastic-scattering data[8] these parameters showed similar ranges of values but the shift was not so well defined as in the SCA analysis.

The lack of agreement, at the most forward angles, between the 2$^+$ angular distributions and both the DWBA and SCA predictions is puzzling. We note, however, that the envelope of the 2$^+$ angular distributions predicted by SCA for 50 MeV α particles (Ref. 5) changes near 25°; it is flatter at more forward angles. The data of Ref. 5 do not extend into this forward angle region nor into the angular region back of ~70°. α-particle data over a larger angular range (i.e., to include smaller and larger angles) would provide a better test of agreement with SCA predictions to compare with the present ^{3}He results. The concept of a single potential with appropriate deformations to fit vibrational and rotational nuclei, as

suggested by the analysis of α-particle data (Ref. 6), is apparently invalid for the present ^{3}He data as can be noted from the trends of the parameters in Table IV. This is in agreement with the analysis of proton data (Ref. 2) and suggests that a single potential can be successfully applied to data (from a range of targets) for a limited angular range only.

Perhaps the best comparison of the present analysis of ^{3}He data with previous studies is the deformation parameters thus obtained. In Fig. 6 values of β_2 obtained in our DWBA and SCA analyses are compared with those from analyses of proton and α-particle scattering and $B(E2)$ measurements. In all cases the β_2 values from the present ^{3}He analyses are larger than from the 50 MeV(p,p') work[2] and in fair agreement with results of $B(E2)$ measurements.[13] There is good consistency of agreement of the values for each isotope from the variety of data used to obtain them. Figure 6 shows a clear trend of a steady increase of β_2 with isotope mass for the vibrational nuclei followed by a larger increase at the transition to rotational nuclei.

In Fig. 7 values of β_3 obtained for the vibrational nuclei are compared. The previously reported value for ^{150}Sm, which was obtained from analysis of proton scattering,[4] is in good agreement with the present ^{3}He analyses. The most surprising behavior of the results presented in Fig. 7 is a decrease of β_3 as the isotope mass increases from 148 to 150. This may imply a change in character of the 3$^-$ level as the isotope mass approaches the transition from vibrational to rotational.

*Operated by Union Carbide Corp., for the U.S. Energy Research and Development Administration.

[1]See AIP document No. PAPS PRVCA-16-1314-9 for 9 pages of tabulated experimental elastic and inelastic cross sections. Order by PAPS number and journal reference from American Institute of Physics, Physics Auxiliary Publication Service, 335 East 45th Street, New York, N.Y. 10017. The price is $1.50 for microfiche and $5.00 for photocopies. Airmail additional. Make checks payable to the American Institute of Physics. This material also appears in *Current Physics Microfilm,* the monthly microfilm edition of the complete set of journals published by AIP, on the frames immediately following this journal article.

[2](a) C. B. Fulmer, F. G. Kingston, A. Scott, and J. C. Hafele, Phys. Lett. 32B, 454 (1970). (b) P. B. Woolam, R. J. Griffiths, F. G. Kingston, C. B. Fulmer, J. C. Hafele, and A. Scott, Nucl. Phys. A179, 659 (1972).

[3]P. Stoler, M. Slagowitz, W. Malcofske, and J. Kruse, Phys. Rev. 155, 1334 (1967).

[4]P. H. Brown and P. Stoler, Phys. Rev. C 2, 765 (1970).

[5]D. L. Hendrie, N. K. Glendenning, B. G. Harvey, O. N. Jarvis, H. H. Duhm, J. Sardinos, and J. Mahoney, Phys. Lett. 26B, 127 (1968).

[6]N. K. Glendenning, D. L. Hendrie, and O. N. Jarvis, Phys. Lett. 26B, 131 (1968).

[7]P. B. Woolam, R. J. Griffiths, and N. M. Clarke, Nucl. Phys. A189, 321 (1972).

[8]R. Eagle, N. M. Clarke, R. J. Griffiths, C. B. Fulmer, and D. C. Hensley, J. Phys. G 1, 358 (1975).

[9]G. Palla and C. Pegel, Z. Phys. 268, 51 (1974).

[10]R. Eagle, R. J. Griffiths, and B. C. Sinha, Phys. Lett. 57B, 31 (1975).

[11]P. D. Kunz, University of Colorado Report No. COO-535-606 (unpublished).

[12]S. A. Weisrose, N. M. Clarke, and R. J. Griffiths, J. Phys. G 1, 334 (1975).

[13]P. H. Stelson and L. Grodzins, Nucl. Data A1, 1 (1965); A. Christy and O. Hausser, *ibid.* A11, 281 (1972).

[14]T. Tamura, Rev. Mod. Phys. 37, 679 (1965); Oak Ridge National Laboratory Report No. ORNL-4152, 1967 (unpublished); private communication. The Karlsruhe version of the code JUPITOR used in the present work is a modification by H. Rebel and G. W. Schweimer.

[15]J. Raynal (unpublished); Features of the program ECIS73 are described in a series of lectures given at the Seminar Course on Computing as a Language of Physics, ICTP, Trieste, August 1971 (unpublished).